

J. H. Khushvaktov^{1,2}, J. Adam^{1,3}, A. A. Baldin^{1,4},
W. I. Furman¹, S. A. Gustov¹, Yu. V. Kish¹,
A. A. Solnyshkin¹, V. I. Stegailov¹, J. Svoboda^{1,5},
P. Tichy¹, V. M. Tsoupko-Sitnikov¹, S. I. Tyutyunnikov¹,
R. Vespalec^{1,6}, J. Vrzalova^{1,3}, V. Wagner³,
B. S. Yuldashev^{1,2}, L. Zavorka¹, M. Zeman^{1,5}

MONTE CARLO SIMULATIONS
AND EXPERIMENTAL RESULTS
ON NEUTRON PRODUCTION
IN THE SPALLATION TARGET **QUINTA**
IRRADIATED WITH 660 MeV PROTONS

Submitted to “Applied Radiation and Isotopes”

¹ Joint Institute for Nuclear Research, Dubna, Russia

² Institute of Nuclear Physics AS RU, Tashkent, Uzbekistan

³ Nuclear Physics Institute CAS, Czech Republic

⁴ Institute for Advanced Studies, Dubna, Russia

⁵ Brno University of Technology, Brno, Czech Republic

⁶ Czech Technical University, Prague, Czech Republic

Хушвактов Ж. Х. и др.

E6-2017-50

Моделирование методом Монте-Карло и экспериментальные результаты по генерации нейтронов в мишени «Квинта», облученной протонами с энергией 660 МэВ

Эксперимент проводился с использованием ускоренного пучка протонов от фазотрона в Объединенном институте ядерных исследований (ОИЯИ). Мишень из природного урана (512 кг) «Квинта» облучалась протонами с энергией 660 МэВ. Моделирование методом Монте-Карло выполнено с использованием кодов FLUKA и Geant4. Определены число утекающих нейтронов из секций урановой мишени, окруженных свинцовой защитой, и число утекающих нейтронов из самой свинцовой защиты. Определено общее число делений внутри мишени «Квинта». Получены экспериментальные значения скоростей реакций для остаточных ядер в образце ^{127}I . Проведено сравнение нескольких значений скоростей реакций с результатами моделирования по кодам FLUKA и Geant4. Экспериментально определенные флюенсы нейтронов, в интервале энергий 10–200 МэВ, с использованием (n, xn) -реакций в образце ^{127}I (NaI) сравниваются с результатами моделирования. Оценена возможность трансмутации долгоживущего радионуклида ^{129}I в установке «Квинта».

Работа выполнена в Лаборатории ядерных проблем им. В. П. Джеллепова ОИЯИ.

Препринт Объединенного института ядерных исследований. Дубна, 2017

Khushvaktov J. H. et al.

E6-2017-50

Monte Carlo Simulations and Experimental Results on Neutron Production in the Spallation Target QUINTA Irradiated with 660 MeV Protons

The activation experiment was performed using the accelerated beam of the Phasotron accelerator at the Joint Institute for Nuclear Research (JINR). The natural uranium spallation target QUINTA was irradiated with protons of energy 660 MeV. Monte Carlo simulations were performed using the FLUKA and Geant4 codes. The number of leakage neutrons from the sections of the uranium target surrounded by the lead shielding and the number of leakage neutrons from the lead shield were determined. The total number of fissions in the setup QUINTA were determined. Experimental values of reaction rates for the produced nuclei in the ^{127}I sample were obtained, and several values of the reaction rates were compared with the results of simulations by the FLUKA and Geant4 codes. The experimentally determined fluence of neutrons in the energy range of 10–200 MeV using the (n, xn) reactions in the ^{127}I (NaI) sample was compared with the results of simulations. Possibility of transmutation of the long-lived radionuclide ^{129}I in the QUINTA setup was estimated.

The investigation has been performed at the Dzhelapov Laboratory of Nuclear Problems, JINR.

Preprint of the Joint Institute for Nuclear Research. Dubna, 2017

1. INTRODUCTION

There is an increasing interest in the application of Accelerator-Driven Systems (ADS) to operate the subcritical nuclear reactors fueled by thorium or natural uranium and to transmute long-lived radioisotopes in spent nuclear fuel into shorter-lived or stable nuclei. High-current, high-energy accelerators or cyclotrons are able to produce neutrons from heavy elements by spallation. A significant number of research facilities which explore this phenomenon already exist, and there are plans for more advanced ones [1–5]. In this process, a beam of high-energy protons (usually $E > 500$ MeV) is directed at a high-atomic-number target (e.g., tungsten, tantalum, depleted uranium, thorium, lead, lead–bismuth) and up to one neutron can be produced per 25 MeV of the incident proton beam energy. A 1000 MeV beam will create 20–30 spallation neutrons per proton. Measurement of fluence of high-energy neutrons is an important task to be investigated. Nuclear reactions, such as (n, xn) reactions, occur only when the neutrons have energies above a particular threshold energy. In many cases, these reactions lead to a production of radioactive nuclei which can be measured after the irradiation. We can use these reactions to determine the fluence or energy spectrum of fast neutrons. In this work we used the $^{127}\text{I}(n, 2n)^{126}\text{I}$, $^{127}\text{I}(n, 4n)^{124}\text{I}$, $^{127}\text{I}(n, 5n)^{123}\text{I}$, $^{127}\text{I}(n, 7n)^{121}\text{I}$, $^{127}\text{I}(n, 8n)^{120}\text{I}$ and $^{127}\text{I}(n, 9n)^{119}\text{I}$ threshold reactions to determine the fluence of fast neutrons. One of the most important aspects of the ADS project needed for the design of the demonstrator is the experimental verification of the simulation. In this paper, we present new experimental data and compare them with the results of simulations performed by the FLUKA [6, 7] and Geant4 [8–10] codes.

2. STRUCTURE OF THE SETUP QUINTA

The uranium assembly QUINTA is presented in Fig. 1. It consists of five sections of hexagonally shaped aluminum containers with an inscribed circle of diameter 28.4 cm. The containers are filled with cylindrical rods of natural uranium, having a sealed aluminum shell (external dimensions: 3.6 cm diameter, 10.4 cm length, and 1.72 kg uranium mass). The containers are made of 5 mm thick aluminum. The first section, facing the proton beam, contains 54 uranium

rods and has a central beam window, 80 mm in diameter, installed in order to reduce its albedo and to reduce the leakage of neutrons from the target. Four

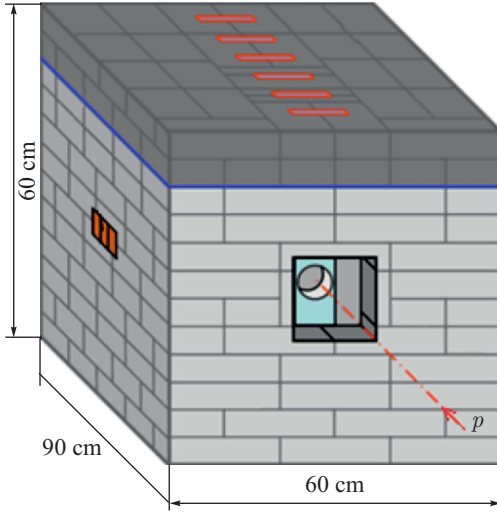


Fig. 1. General view of the QUINTA setup

subsequent sections are structurally identical and each section contains 61 uranium rods. The mass of the natural uranium in each of these sections is 104.92 kg, and the total mass of uranium in the entire target is 512.56 kg. The void filling factor of the 2nd, 3rd, 4th, and 5th uranium sections is about 0.8, and that of the entire assembly is 0.6. The uranium target is surrounded with a lead shielding of 10-cm thickness and a weight of 2545 kg and with a beam entrance window of the dimensions of 15×15 cm. There is a window of the 15×15 cm size in the side wall of the shielding near the third section, where the exper-

imental samples can be placed. The upper part of the lead assembly has a special hole for mounting and dismantling of experimental samples as well as for their installation inside the uranium assembly between sections.

3. EXPERIMENT

During the experiment $^{127}\text{I}(\text{NaI})$ and $^{129}\text{I}(\text{NaI})$ samples were placed inside the window on the left side of the QUINTA setup (see Fig. 1). Masses of the ^{23}Na and ^{127}I isotopes in the ^{127}I sample are respectively 0.23 g and 1.27 g, and masses of the ^{23}Na and ^{129}I in the ^{129}I sample are respectively 0.067 g and 0.339 g. The total number of incident protons colliding with the target was determined by the standard method of activation of aluminum foil by the reaction $^{27}\text{Al}(p, x)^{24}\text{Na}$. At the end of the irradiation lasting 300 min, the total number of incident protons was $2.4(3)\text{E} + 15$. The γ -ray spectra of the samples were measured using the Canberra HPGe detector with a relative efficiency of 19% and the energy resolution of 1.8 keV at the 1.33 MeV ^{60}Co line. Energy and efficiency calibrations of the detectors were performed using a set of the γ -ray standards (^{54}Mn , ^{57}Co , ^{60}Co , ^{88}Y , ^{113}Sn , ^{133}Ba , ^{137}Cs , ^{139}Ce , ^{152}Eu , ^{228}Th , ^{241}Am). We measured nine γ -ray spectra with different time durations, and the cooling time of the first spectrum is

32 min. The initial analysis of the measured γ -ray spectra was performed using the DEIMOS32 code [11]. The program allows one to determine the areas under the peaks and their positions (channel number). After that, by using a software package [12], the spectra were calibrated for energy and corrected for the detector efficiency, and separate γ -ray lines of the produced nuclei were identified as they were produced in the samples as a result of interactions with secondary neutrons. Experimental count rates of the individual γ -ray transitions were corrected for the nuclear decay during the irradiation as well as for the self-absorption of the γ -rays measured, and for the true coincidence summing [13]. All these procedures are described in detail in [12, 14, 15]. For determining the experimental reaction rates, the following equation was used [15]:

$$R(A_r, Z_r) = \frac{Q(A_r, Z_r)}{N_t N_p}, \quad (1)$$

where $Q(A_r, Z_r)$ is the production rate of the radioactive nucleus (A_r, Z_r) , N_t the number of atoms in the sample, and N_p the number of incident protons on the target.

4. MONTE CARLO SIMULATIONS

The FLUKA hadron–nucleon interaction models are based on resonance production and decay at energies below a few GeV, and on the Dual Parton model at energies above. Two models are also used in hadron–nucleus interactions. At momenta below 3–5 GeV/ c the PEANUT package [16, 17] includes a very detailed Generalised IntraNuclear Cascade (GINC) and a pre-equilibrium stage, while at high energies the Gribov–Glauber multiple collision mechanism is included in a less refined GINC. Both modules are followed by equilibrium processes: evaporation, fission, Fermi break-up, γ -ray de-excitation [18, 19]. Transport of neutrons with energies lower than a certain energy is performed in FLUKA by a multigroup algorithm. The energy boundary below which multigroup transport takes over depends in principle on the cross section library used. In the FLUKA neutron cross section library, the energy range up to 20 MeV is divided into 260 energy groups of approximately equal logarithmic width (31 of which are thermal).

The Bertini Intranuclear Cascade Model in Geant4 is a re-engineered version of the INUCL code [20] and includes the Bertini intranuclear cascade model with excitons, a pre-equilibrium model, a nucleus explosion model, a fission model, and an evaporation model. It treats nuclear reactions initiated by long-lived hadrons (p , n , π , K , Λ , Σ , Ξ , Ω) and γ 's with energies between 0 and 10 GeV. In the simulations by the Geant4 code, the neutron transport class library simulates the interactions of neutrons with kinetic energies from thermal energies up to 20 MeV. The interactions of neutrons at low energies are split into four parts

in analogy to the other hadronic processes in Geant4. Radiative capture, elastic scattering, fission, and inelastic scattering are considered as separate models. All cross-section data are taken from the ENDF/B-VI [21] evaluated data library. The high-precision (HP) neutron models depend on the evaluated neutron data library (G4NDL) of cross sections, angular distributions and final state information and used when data are found in the library. When data are missing, low-energy parameterized neutron models are used and these alternative models cover the same types of interaction as the originals, that is, elastic and inelastic scattering, capture and fission.

5. RESULTS AND DISCUSSION

Neutron leakage energy spectra have been obtained in the simulations by the FLUKA and Geant4 codes. Figure 2 shows the spectra of leakage neutrons from the natural uranium assembly (included backscattered neutrons from the lead shielding) and from the lead shielding. Simulated neutron energy spectra have a good agreement, excluding low energy region (up to 1 keV). By FLUKA simulations the total number of leakage neutrons from the sections of natural uranium target is 144 and by Geant4 simulations it is 134 neutrons per proton. The total number of leakage neutrons from the lead shielding is respectively 38 and 44 neutrons per one incident proton.

The results of simulations also provide detailed information about the number of fissions in each natural uranium cylinder of the QUINTA setup. Table 1 gives results of simulations by the FLUKA code about the number of fissions for natu-

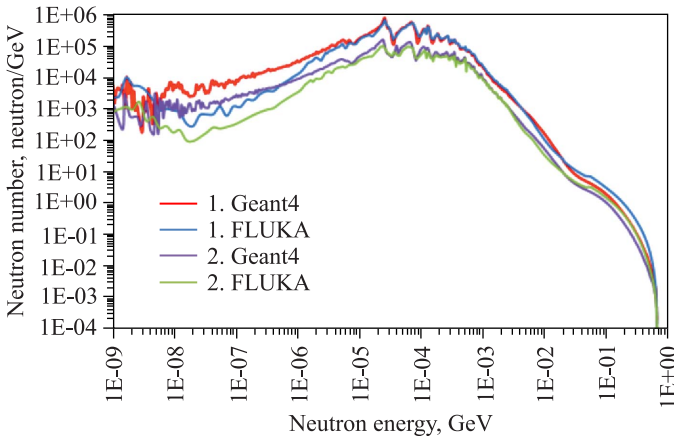


Fig. 2. Energy spectrum of leakage neutrons from the natural uranium assembly (1) and from the lead shielding (2)

Table 1. Number of fissions for natural uranium cylinders per one 660 MeV proton

No. of U bars	Section No. 1	Section No. 2	Section No. 3	Section No. 4	Section No. 5
U01	4.15E-03	6.88E-03	7.07E-03	4.11E-03	1.86E-03
U02	5.25E-03	9.18E-03	9.31E-03	5.01E-03	1.96E-03
U03	6.09E-03	1.12E-02	1.06E-02	5.32E-03	2.14E-03
U04	6.46E-03	1.13E-02	1.02E-02	5.07E-03	2.03E-03
U05	5.83E-03	9.60E-03	8.45E-03	4.33E-03	1.88E-03
U06	4.84E-03	8.07E-03	8.43E-03	4.81E-03	2.03E-03
U07	6.97E-03	1.26E-02	1.25E-02	6.33E-03	2.47E-03
U08	8.81E-03	1.81E-02	1.64E-02	7.48E-03	2.61E-03
U09	1.03E-02	2.16E-02	1.78E-02	7.52E-03	2.67E-03
U10	1.03E-02	1.93E-02	1.54E-02	6.50E-03	2.38E-03
U11	7.99E-03	1.31E-02	1.09E-02	5.05E-03	2.02E-03
U12	4.87E-03	8.42E-03	8.80E-03	5.04E-03	2.04E-03
U13	8.04E-03	1.46E-02	1.47E-02	7.29E-03	2.54E-03
U14	1.26E-02	2.57E-02	2.38E-02	1.00E-02	3.12E-03
U15	1.70E-02	4.13E-02	3.25E-02	1.14E-02	3.36E-03
U16	2.00E-02	4.65E-02	2.99E-02	1.01E-02	3.18E-03
U17	1.61E-02	2.94E-02	2.00E-02	7.53E-03	2.58E-03
U18	9.78E-03	1.64E-02	1.24E-02	5.45E-03	2.12E-03
U19	4.62E-03	7.67E-03	7.95E-03	4.64E-03	2.03E-03
U20	7.67E-03	1.37E-02	1.40E-02	7.10E-03	2.59E-03
U21	1.36E-02	2.73E-02	2.61E-02	1.14E-02	3.17E-03
U22		6.34E-02	6.00E-02	2.06E-02	4.45E-03
U23		1.86E-01	8.71E-02	1.76E-02	4.09E-03
U24	9.11E-02	9.13E-02	4.12E-02	1.13E-02	3.18E-03
U25	2.09E-02	3.45E-02	2.12E-02	7.83E-03	2.46E-03
U26	9.91E-03	1.57E-02	1.19E-02	5.16E-03	2.05E-03
U27	3.82E-03	6.04E-03	6.33E-03	4.00E-03	1.76E-03
U28	6.32E-03	1.07E-02	1.12E-02	5.96E-03	2.34E-03
U29	1.18E-02	2.07E-02	2.06E-02	9.42E-03	2.98E-03
U30		4.75E-02	4.76E-02	1.71E-02	3.78E-03
U31		2.60E-01	1.95E-01	2.64E-02	4.60E-03
U32		6.08E-01	9.88E-02	1.62E-02	3.96E-03
U33	8.03E-02	7.39E-02	3.34E-02	9.98E-03	2.91E-03
U34	1.62E-02	2.56E-02	1.69E-02	6.57E-03	2.31E-03
U35	7.87E-03	1.15E-02	9.41E-03	4.38E-03	1.83E-03
U36	4.63E-03	7.42E-03	8.09E-03	4.74E-03	2.00E-03
U37	7.62E-03	1.40E-02	1.40E-02	7.02E-03	2.58E-03
U38	1.34E-02	2.72E-02	2.60E-02	1.14E-02	3.20E-03
U39		6.33E-02	5.98E-02	2.07E-02	4.52E-03
U40		1.85E-01	8.65E-02	1.77E-02	3.96E-03
U41	9.06E-02	9.15E-02	4.11E-02	1.15E-02	3.20E-03
U42	2.09E-02	3.45E-02	2.12E-02	7.87E-03	2.55E-03

Table 1 (continued)

No. of U bars	Section No. 1	Section No. 2	Section No. 3	Section No. 4	Section No. 5
U43	9.87E-03	1.53E-02	1.17E-02	5.01E-03	2.09E-03
U44	4.97E-03	8.52E-03	8.68E-03	4.95E-03	2.07E-03
U45	8.16E-03	1.48E-02	1.44E-02	7.33E-03	2.63E-03
U46	1.26E-02	2.60E-02	2.34E-02	1.01E-02	3.11E-03
U47	1.68E-02	4.16E-02	3.28E-02	1.16E-02	3.34E-03
U48	1.96E-02	4.61E-02	2.98E-02	1.01E-02	3.10E-03
U49	1.61E-02	2.93E-02	1.99E-02	7.59E-03	2.51E-03
U50	1.00E-02	1.61E-02	1.23E-02	5.38E-03	2.07E-03
U51	4.81E-03	8.10E-03	8.18E-03	4.69E-03	1.99E-03
U52	6.87E-03	1.27E-02	1.24E-02	6.19E-03	2.36E-03
U53	8.71E-03	1.78E-02	1.61E-02	7.47E-03	2.56E-03
U54	1.03E-02	2.14E-02	1.77E-02	7.50E-03	2.55E-03
U55	1.02E-02	1.94E-02	1.54E-02	6.60E-03	2.37E-03
U56	7.85E-03	1.29E-02	1.09E-02	5.07E-03	1.98E-03
U57	4.07E-03	6.69E-03	6.99E-03	4.00E-03	1.81E-03
U58	5.13E-03	9.06E-03	9.02E-03	4.83E-03	2.05E-03
U59	6.13E-03	1.10E-02	1.03E-02	5.21E-03	2.05E-03
U60	6.30E-03	1.12E-02	1.02E-02	4.95E-03	2.01E-03
U61	5.82E-03	9.48E-03	8.43E-03	4.34E-03	1.85E-03

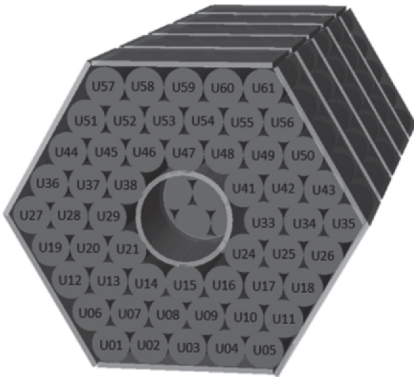


Fig. 3. Marking of ^{235}U bars of the QUINTA setup for the definition of fission numbers

ral uranium cylinders per one 660 MeV proton. Marking of the cylinders is shown in Fig. 3. The total number of fissions in the setup generated by one 660 MeV proton is 5.52, and 1.65 fissions of them are generated with high-energy ($E > 20$ MeV) particles. From the fissions with high-energy ($E > 20$ MeV) particles, 0.79 fissions are generated by protons, 0.84 fissions are generated by neutrons, $5.59 \cdot 10^{-3}$ fissions are generated by the positive pions and $1.08 \cdot 10^{-2}$ fissions are generated by the negative pions. The total number of fissions per incident proton is 0.75 in the 1st section, 2.59 in the 2nd section, 1.51 in the 3rd section, 0.51 in the 4th section and 0.16 in the 5th section. The number of fissions with high-energy ($E > 20$ MeV) particles is 0.18 in the 1st section, 0.84 in the 2nd section, 0.46 in the 3rd section, 0.13 in the 4th section and 0.04 in the 5th section.

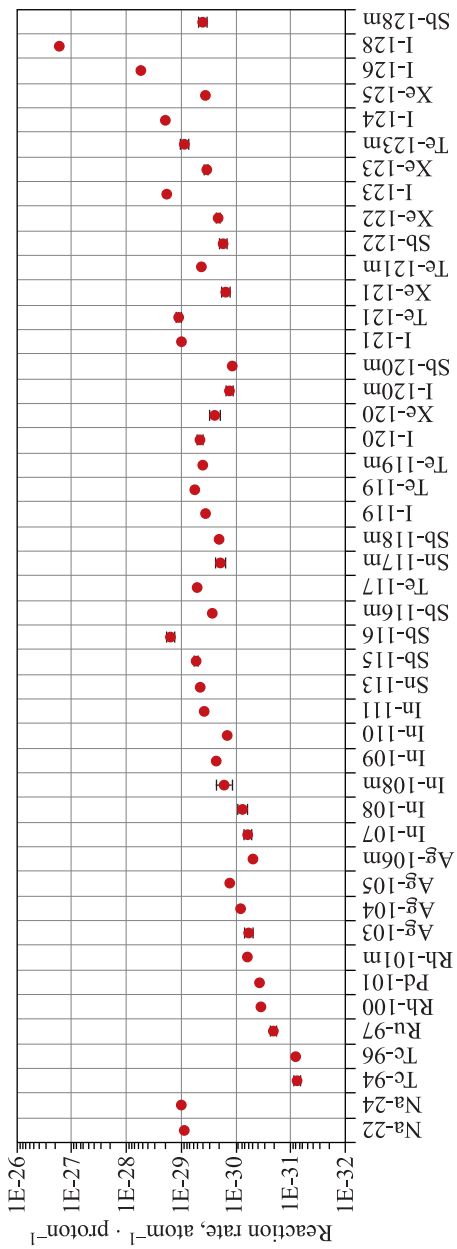


Fig. 4. Cumulative reaction rates for residual radionuclides in the sample $^{127}\text{I}(\text{NaI})$

Figure 4 shows cumulative experimental reaction rates for the residual radionuclides produced in the $^{127}\text{I}(\text{NaI})$ sample. Among the identified radionuclides ^{24}Na and ^{22}Na are produced in the reactions $^{23}\text{Na}(n, \gamma)^{24}\text{Na}$ and $^{23}\text{Na}(n, 2n)^{22}\text{Na}$. Table 2 gives the independent values of reaction rates for products of the reactions $^{127}\text{I}(n, \gamma)$ and $^{127}\text{I}(n, xn)$ and comparison with the results of simulations. The independent values of reaction rates for the ^{123}I , ^{121}I , and ^{120}I radionuclides are determined by considering the number of the ^{123}Xe , ^{121}Xe and ^{120}Xe radionuclides, identified in the experiment and for ^{119}I used from the ratio of produced ^{120}I to ^{120}Xe . The radionuclides ^{128}I , ^{126}I and ^{124}I cannot be produced via β^+ decay or electron capture, and therefore we obtained the independent values of reaction rates in the experiment. The results of simulations for the $^{127}\text{I}(n, xn)$ reactions are in good agreement with the experimental results. We assume that for the $^{127}\text{I}(n, \gamma)$ reaction the difference between the results of simulations and

Table 2. Independent values of reaction rates for the products of the reactions $^{127}\text{I}(n, \gamma)$ and $^{127}\text{I}(n, xn)$ and comparison with the results of simulations

Nuclear reaction	Experimental reaction rate	Exp./Calc. (FLUKA)	Exp./Calc. (Geant4)
$^{127}\text{I}(n, \gamma)^{128}\text{I}$	1.68(9)E-27	0.36(1)	0.21(1)
$^{127}\text{I}(n, 2n)^{126}\text{I}$	5.28(23)E-29	1.02(4)	0.41(2)
$^{127}\text{I}(n, 4n)^{124}\text{I}$	1.86(4)E-29	1.14(2)	0.90(2)
$^{127}\text{I}(n, 5n)^{123}\text{I}$	1.50(8)E-29	1.19(6)	0.91(5)
$^{127}\text{I}(n, 7n)^{121}\text{I}$	8.43(36)E-30	2.71(12)	1.34(6)
$^{127}\text{I}(n, 8n)^{120}\text{I}$	1.77(18)E-30	1.42(14)	0.69(7)
$^{127}\text{I}(n, 9n)^{119}\text{I}$	1.47(14)E-30	1.89(18)	1.04(10)

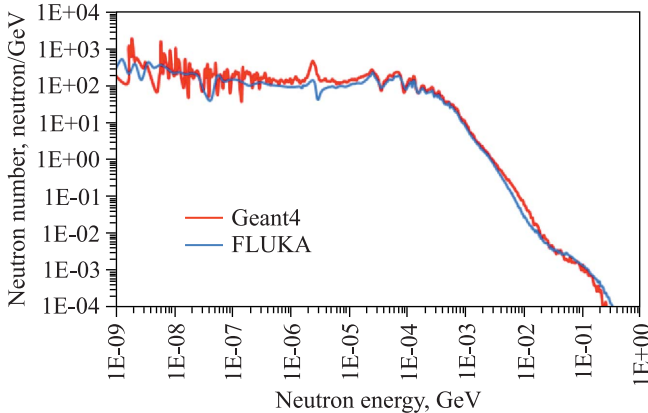


Fig. 5. Energy spectrum of neutrons in the sample $^{127}\text{I}(\text{NaI})$

experiment is caused by insufficient statistics for the accurate determination of the low-energy (up to 1 keV) neutron fluence, which have a high capture cross section for the ^{127}I nuclei. The simulated neutron energy spectra in the sample $^{127}\text{I}(\text{NaI})$ are shown in Fig. 5, and the results of both the codes are in good agreement.

For experimental determination of the neutron fluence we used 80% of the experimental independent values of reaction rates, because the results of simulations by the FLUKA code show that neutrons in the energy interval ΔE add 80(3)% contribution to the reaction rate. Dependencies of (n, xn) reaction rates on the energy of secondary neutrons in the sample $^{127}\text{I}(\text{NaI})$ are shown in Fig. 6. The neutron fluence is defined by solving equation (2). The averaged values of

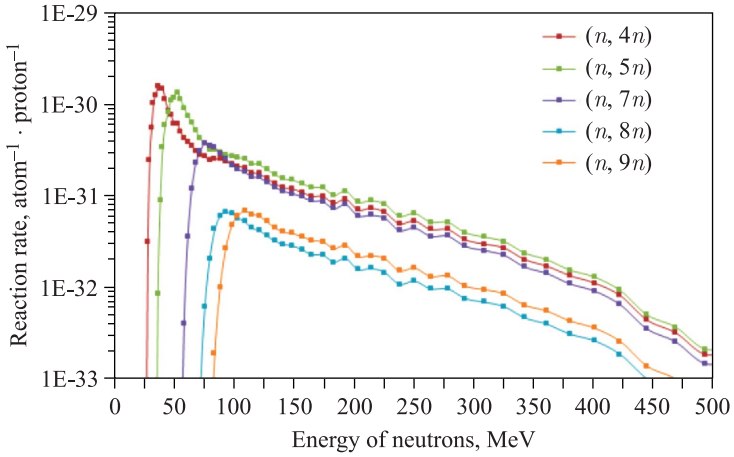


Fig. 6. Dependencies of some $^{127}\text{I}(n, xn)$ reaction rates on energy of neutrons

Table 3. Detailed table for the determination of the neutron fluence using the $^{127}\text{I}(n, xn)$ reactions. $0.8R$ — 80% of independent values of reaction rate $R(\text{exp.})$, σ — averaged values of reaction cross sections for energy interval ΔE , φ — fluence of neutrons ($n/\text{MeV} \cdot \text{p} \cdot \text{cm}^2$)

Nuclear reaction	$0.8R$	ΔE , MeV	σ , b	φ
$^{127}\text{I}(n, 2n)^{126}\text{I}$	4.23(19)E-29	10–30	0.668	3.16(63)E-6
$^{127}\text{I}(n, 4n)^{124}\text{I}$	1.49(3)E-29	30–80	0.306	9.7(19)E-7
$^{127}\text{I}(n, 5n)^{123}\text{I}$	1.20(7)E-29	40–90	0.282	8.5(17)E-7
$^{127}\text{I}(n, 7n)^{121}\text{I}$	6.75(29)E-30	65–140	0.105	8.5(17)E-7
$^{127}\text{I}(n, 8n)^{120}\text{I}$	1.42(14)E-30	80–180	0.021	6.8(14)E-7
$^{127}\text{I}(n, 9n)^{119}\text{I}$	1.17(11)E-30	90–200	0.023	4.62(92)E-7

the cross sections for the energy interval ΔE are obtained from the results of simulations by the FLUKA code:

$$R(A_r, Z_r) = \int_{E_{\text{thr}}(A_r, Z_r)}^{E_{\text{max}}} \sigma(A_r, Z_r, E_n) \varphi(E_n) dE_n, \quad (2)$$

where $\sigma(A_r, Z_r, E_n)$ is the reaction cross section and $\varphi(E_n)$ the neutron fluence. Table 3 gives detailed information for the determination of neutron fluence, and Fig. 7 shows the fluence of neutrons in the sample $^{127}\text{I}(\text{NaI})$ for the energy range

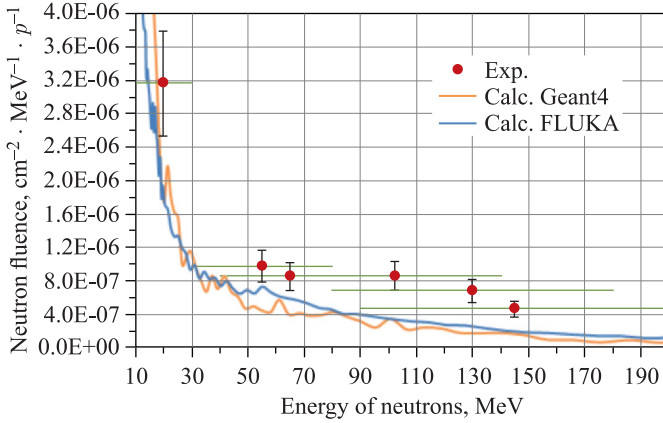


Fig. 7. Fluence of neutrons in the sample $^{127}\text{I}(\text{NaI})$ (with green lines showing energy intervals ΔE , where values of the cross sections were averaged)

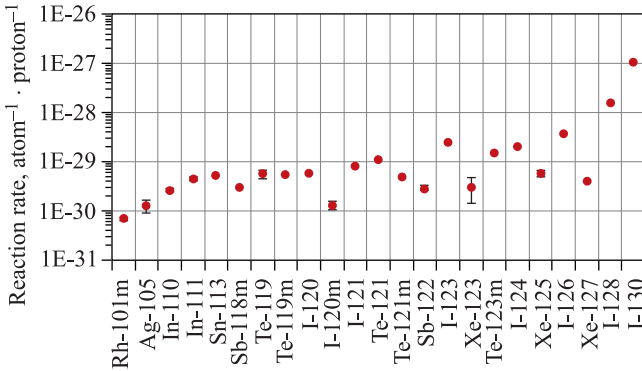


Fig. 8. Cumulative reaction rates for residual radionuclides in the sample $^{129}\text{I}(\text{NaI})$

of 10–200 MeV determined in experiment using the $^{127}\text{I}(n, xn)$ reactions and results of simulations.

The results of simulation show that the capture of neutrons represents 92(2)% of the total interactions of neutrons with nuclei ^{129}I (except elastic scattering) in the $^{129}\text{I}(\text{NaI})$ sample. Ratio of the mass of produced ^{130}I to the mass of ^{129}I is determined, in order to experimentally assess the possibility of transmutation by the $^{129}\text{I}(n, \gamma)$ reaction. The ratio is $2.59(4)\text{E-}12$ for the case of 5-hour irradiation time with $1.33\text{E}+11$ proton/s beam intensity. Figure 8 shows the cumulative reaction rates for residual radionuclides in the $^{129}\text{I}(\text{NaI})$ sample obtained from the experiment.

6. CONCLUSIONS

The natural uranium spallation target QUINTA was irradiated with protons of energy 660 MeV. The simulations were performed by the FLUKA and Geant4 codes. The results of simulations by the FLUKA and Geant4 codes on the leakage of neutrons from the sections of uranium assembly and from the surface of the QUINTA setup are in good agreement. In the case of the $^{127}\text{I}(\text{NaI})$ sample, ratios of the experimental reaction rates to results of simulations by the FLUKA and Geant4 codes for the (n, γ) reaction are 0.36 and 0.21, and for the (n, xn) reactions they are in the range of 0.41–2.71. The results obtained for the determination of neutron fluence, using $^{127}\text{I}(n, xn)$ reactions in the experiment, are in reasonable agreement with the neutron spectra obtained from simulations by the FLUKA and Geant4 codes.

REFERENCES

1. *Furman W. I., Adam J., Baldin A. et al.* Recent Results of the Study of ADS with 500 kg Natural Uranium Target Assembly QUINTA Irradiated by Deuterons with Energies from 1 to 8 GeV at JINR Nuclotron // Proc. of Science, XXI International Baldin Seminar on High Energy Physics Problems, September 10–15, 2012, Dubna, PoS (Baldin ISHEP XXI)086; <http://pos.sissa.it/archive/conferences/173/086/Baldin%20ISHEPP%20XXI.086.pdf>
2. *Sidorin S. F., Rogov A. D., Ponomarev L. I., and Koptelov E. A.* Proposal of the ADS Research Stand Based on the Linac of the Institute for Nuclear Research of the Russian Academy of Sciences // Thorium Energy for the World. 2016. P. 311–326; http://link.springer.com/chapter/10.1007/978-3-319-26542-1_46
3. *Degweker S. B., Singh Pitamber, Satyamurthy P., and Sinha Amar.* Accelerator-Driven Systems for Thorium Utilization in India // Thorium Energy for the World. 2016. P. 333–340; http://link.springer.com/chapter/10.1007/978-3-319-26542-1_48
4. <http://myrrha.sckcen.be/en/MYRRHA/ADS>

5. Yang L., Zhan W.L. New Concept for ADS Spallation Target: Gravity-Driven Dense Granular Flow Target // *Sci. China Tech. Sci.* 2015. V. 58. P. 1705–1711; <http://link.springer.com/article/10.1007/s11431-015-5894-0>
6. Ferrari A., Sala P. R., Fassó A., Ranft J. FLUKA: A Multi-Particle Transport Code. CERN-2005-10 (2005), INFN/TC_05/11, SLAC-R-773; <http://slac.stanford.edu/pubs/slacreports/reports16/slac-r-773.pdf>
7. Böhlen T. T., Cerutti F., Chin M. P. W., Fassó A., Ferrari A., Ortega P. G., Mairani A., Sala P. R., Smirnov G., and Vlachoudis V. The FLUKA Code: Developments and Challenges for High Energy and Medical Applications // *Nucl. Data Sheets.* 2014. V. 120. P. 211–214; <http://dx.doi.org/10.1016/j.nds.2014.07.049>
8. Agostinelli S., Allison J., Amako K. et al. Geant4 — a Simulation Toolkit // *Nucl. Instr. Meth. A.* 2003. V. 506. P. 250–303; [http://dx.doi.org/10.1016/S0168-9002\(03\)01368-8](http://dx.doi.org/10.1016/S0168-9002(03)01368-8)
9. Allison J., Amako K., Apostolakis J. et al. Geant4 Developments and Applications // *IEEE Trans. Nucl. Sci.* 2006. V. 53, No. 1. P. 270–278; <http://ieeexplore.ieee.org/stamp/stamp.jsp?arnumber=1610988>
10. Allison J., Amako K., Apostolakis J. et al. Recent Developments in Geant4 // *Nucl. Instr. Meth. A.* 2016. V. 835. P. 186–225; <http://dx.doi.org/10.1016/j.nima.2016.06.125>
11. Frana J. Program DEIMOS32 for Gamma-Ray Spectra Evaluation // *J. Radioanal. Nucl. Chem.* 2003. V. 257, No. 3. P. 583–587; <http://link.springer.com/article/10.1023%2FA%3A1025448800782>
12. Adam J., Pronskikh V. S., Balabekyan A. R., Kalinnikov V. G., Mrazek J., Priemishev A. N., Frana J. Program Package and Supplements to Activation Analysis for Calculations of Nuclear Reaction Cross Sections. JINR Preprint P10-2000-28. Dubna, 2000; <http://www1.jinr.ru/Preprints/2000/p10-2000-28.pdf>
13. Sudár S. “TRUECOINC”, a Software Utility for Calculation of the True Coincidence Correction. IAEA-TECDOC-1275. P. 37–48; http://www.iaea.org/inis/collection/NCLCollectionStore/_Public/33/017/33017174.pdf?r=1
14. Adam J., Balabekyan A. R., Barashenkov V. S. et al. Study of Product Formation in Proton–Nuclear Reactions on the ^{129}I Target Induced by 660 MeV Protons // *Part. Nucl., Lett.* 2004. V. 1, No. 4(121). P. 53–64; http://www1.jinr.ru/Pepan_letters/panl_4_2004/06_adam.pdf
15. Adam J., Katovsky K., Majerle M., Krivopustov M. I., Kumar V., Bhatia Chitra, Sharma Manish, Solnyshkin A. A., Tsoumpko-Sitnikov V. M. A Study of Nuclear Transmutation of Th and ^{235}U with Neutrons Produced in Pb Target and U Blanket Irradiated by 1.6 GeV Deuterons // *Eur. Phys. J. A.* 2010. V. 43. P. 159–173; JINR Preprint E15-2008-118, Dubna, 2008; <http://link.springer.com/article/10.1140/epja/i2010-10909-y>
16. Ferrari A., Sala P. R. A New Model for Hadronic Interactions at Intermediate Energies for the FLUKA Code // *Proc. MC93 Intern. Conf. on Monte Carlo Simulation in High Energy and Nuclear Physics.* Tallahassee (Florida), 22–26 February 1993 / Ed. by P. Dragovitsch, S. L. Linn, M. Burbank. Singapore: World Sci., 1994. P. 277–288; http://www.fluka.org/content/publications/1993_mc_preq.pdf

17. *Ferrari A., Sala P.R.* The Physics of High Energy Reactions // Proc. Workshop on Nuclear Reaction Data and Nuclear Reactors Physics, Design and Safety, International Centre for Theoretical Physics, Miramare-Trieste, Italy, 15 April–17 May 1996; http://www.fluka.org/content/publications/1996_trieste.pdf
18. *Ferrari A., Ranft J., Roesler S., Sala P.R.* The Production of Residual Nuclei in Peripheral High Energy Nucleus–Nucleus Interactions // *Z. Phys. C.* 1996. V. 71. P. 75–86; <http://link.springer.com/article/10.1007%2Fs002880050149>
19. *Ferrari A., Ranft J., Roesler S., Sala P.R.* Cascade Particles, Nuclear Evaporation, and Residual Nuclei in High Energy Hadron–Nucleus Interactions // *Z. Phys. C.* 1996. V. 70. P. 413–426; <http://link.springer.com/article/10.1007%2Fs002880050119>
20. *Titarenko Yu.E., Shvedov O.V., Batyaev V.F., Karpikhin E.I., Zhivun V.M., Mulfambetov R.D., Sosnin A.N., Mashnik S.G., Prael R.E., Gabriel T.A., Blann M.* Experimental and Computer Simulations Study of Radionuclide Production in Heavy Materials Irradiated by Intermediate Energy Protons. nucl-ex/9908012. 1999; <https://arxiv.org/abs/nucl-ex/9908012>
21. ENDF/B-VI: Cross Section Evaluation Working Group, ENDF/B-VI Summary Document, Report BNL-NCS-17541 (ENDF-201) / Ed. by P.F.Rose, National Nuclear Data Center, Brookhaven National Laboratory, Upton, NY, USA, 1991; http://www.iaea.org/inis/collection/NCLCollectionStore/_Public/23/060/23060878.pdf

Received on July 10, 2017.

Редактор *Е. И. Кравченко*

Подписано в печать 04.09.2017.

Формат 60 × 90/16. Бумага офсетная. Печать офсетная.

Усл. печ. л. 1,0. Уч.-изд. л. 1,37. Тираж 215 экз. Заказ № 59224.

Издательский отдел Объединенного института ядерных исследований

141980, г. Дубна, Московская обл., ул. Жолио-Кюри, 6.

E-mail: publish@jinr.ru

www.jinr.ru/publish/